Optical characterization of structure for semiconductor quantum dots

Weidong Sheng
Department of Physics, Fudan University, Shanghai 200433, People's Republic of China
and Department of Physics, The University of Hong Kong, Pokfulam Road, Hong Kong, People's Republic of China

S. J. Xu
Department of Physics, The University of Hong Kong, Pokfulam Road, Hong Kong, People's Republic of China
(Received 10 December 2007; revised manuscript received 14 January 2008; published 12 March 2008)

Linear polarization of the multiexciton emission from self-assembled quantum dots is investigated by using an empirical tight-binding method. The polarization of the primary interband transition is shown to have a quadratic dependence on the lateral aspect ratio of the structures and is insensitive to both the excitonic and random intermixing effects, which make it an appropriate tool for structure characterization. The ground-state transitions in the emission spectra of multiexciton complexes are found to exhibit very different polarization from the primary interband transition, which we attribute to different component profiles in the excited valence-band states.

DOI: 10.1103/PhysRevB.77.113305 PACS number(s): 78.67.Hc, 68.65.Hb, 73.21.La

Semiconductor self-assembled quantum dots, sometimes called artificial atoms,[1] are three-dimensional nanostructures in which carriers are confined along the three dimensions of space by the band gap difference between the dot and barrier materials. The electronic and optical properties of these nanoscale systems are affected by the strong influence of the low symmetry of the confined nanostructures and the strain due to the lattice mismatch between the different materials. Unlike natural atoms, self-assembled quantum dots take various shapes that can be either symmetric or asymmetric. Ascertaining the shape of quantum dots and other related structural parameters is of primary importance for both fundamental and practical reasons.[2]

In the absence of magnetic field, the emission from quantum dots is often not isotropic with respect to its polarization direction.[3,4] Strong biaxial strain suppresses light-hole components in the valence-band states, leaving mostly heavy-hole components and resulting in in-plane polarized emission from the interband transitions.[5,6] It has been shown that the linear polarization of the interband transitions in a self-assembled quantum dot originates from its shape anisotropy.[7] Due to very little difference in the dielectric constants between the quantum dot and barrier materials, the local field or depolarization effect is believed to contribute only a small portion of the overall linear polarization of the emission.

Optical spectroscopy has been shown to be an appropriate tool for probing many electronic properties of quantum dots, such as the shell structure of electronic states.[8] However, for self-assembled quantum dots, a direct manifestation of geometrical anisotropy by optical spectroscopy has yet been well established, which we believe is due to the lack of an applicable theory that bridges these two aspects. In the present work, we will explore the possibility of optical characterization of structure for semiconductor self-assembled quantum dots. The proposed scheme is based on a quantitative relation established between the optical and shape anisotropies by an empirical tight-binding approach.[9,10]

The model system is an InAs/GaAs quantum dot which is elongated along the $[1\bar{1}0]$ direction. It has a variable lateral aspect ratio $\beta=d_x/d_y$ where d_x $(=d)$ and d_y are the dimensions along the long $(x=[1\bar{1}0])$ and short $(y=[110])$ axes of the structure, respectively. The dot is lens shaped at $\beta=1$ and becomes domelike when it is elongated. The degree of elongation can be varied by changing d_y while keeping d_x fixed.

The photoluminescence from a quantum dot is composed of emission from individual multiexciton complexes. In a N-exciton state, the recombination of one electron-hole pair gives rise to an emission spectrum $I_{\mathbf{e}}(\omega)$ which is given by[11]

$$I_{\mathbf{e}}(\omega)=\sum_{i,f}|\langle C_{N-1}^{f}|\mathbf{P}_{\mathbf{e}}^{-}|C_{N}^{i}\rangle|^2\cdot\delta(E_N^i-E_{N-1}^f-\hbar\omega), \quad (1)$$

where $\mathbf{e}$ denotes the polarization direction ($[1\bar{1}0]$ or $[110]$), C_N^i is the ith eigenstate of the N-exciton system, and E_N^i is the corresponding energy. $\mathbf{P}_{\mathbf{e}}^{-}$ is the recombination operator which is given by

$$\mathbf{P}_{\mathbf{e}}^{-}=\sum_{i,j}p_{ij}(\mathbf{e})\hat{h}_i\hat{c}_j=\sum_{i,j}\langle\Psi_h^i|\mathbf{e}\cdot\hat{\mathbf{p}}|\Psi_e^j\rangle\hat{h}_i\hat{c}_j. \quad (2)$$

Recombination of an electron-hole pair in a single exciton state gives rise to two emission lines which originally are circularly polarized and become almost 100% linearly polarized[12,13] due to the electron-hole exchange interaction which induces a splitting of about 10 μeV.[14] For a multiexciton of higher order, its emission spectrum generally consists of many separated transitions. For one emission line or several lines which have very close energies, the linear polarization can be defined by

$$P_{ex}=\frac{\int I_x(\omega)d\omega-\int I_y(\omega)d\omega}{\int I_x(\omega)d\omega+\int I_y(\omega)d\omega}, \quad (3)$$

where $I_x(\omega)$ and $I_y(\omega)$ are the intensities of emission polarized along the x and y directions, respectively.

Neglecting the electron-hole interaction, the linear polarization of the emission from noninteracting electron-hole pairs is defined by[7]

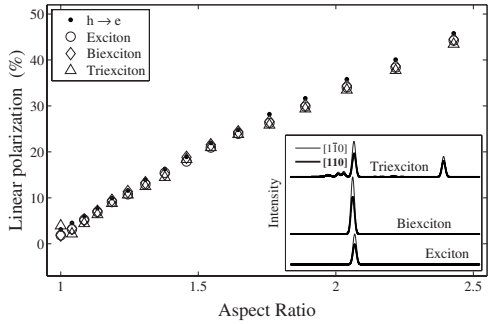

FIG. 1. Linear polarization of the emission from a noninteracting electron-hole pair, single exciton, biexciton, and triexciton in an elongated InAs/GaAs self-assembled quantum dot. Inset: the emission spectra from the multiexciton complexes.

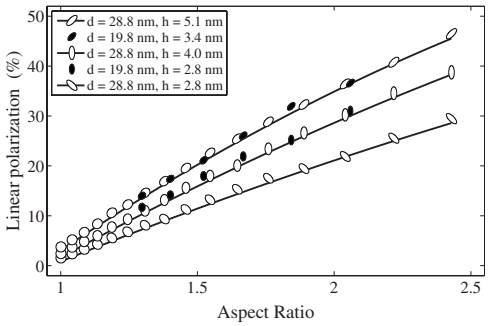

FIG. 2. Linear polarization of the primary interband transition, P_{eh} in dotted lines, calculated as a function of the aspect ratio of the quantum dots with various lateral sizes and heights. The shape and size of the symbols correspond to the denoted structures. Quadratic fit is shown in solid lines.

$$P_{eh} = \frac{|\langle \Psi_e^g | \hat{p}_x | \Psi_h^g \rangle|^2 - |\langle \Psi_e^g | \hat{p}_y | \Psi_h^g \rangle|^2}{|\langle \Psi_e^g | \hat{p}_x | \Psi_h^g \rangle|^2 + |\langle \Psi_e^g | \hat{p}_y | \Psi_h^g \rangle|^2}, \tag{4}$$

where Ψ_e^g (Ψ_h^g) is the ground electronic (hole) state.

Figure 1 plots P_{eh} and several P_{ex} calculated as a function of the aspect ratio of the quantum dots. The height (h) and dimension along the long axis of the dots (d) are chosen as 4.5 and 28.8 nm, respectively. The polarization-dependent emission spectra of the single exciton, biexciton, and triexciton are shown in the inset for a dot of an aspect ratio of $\beta = 1.55$.

The calculation shows that $P_{eh}(\beta)$, $P_X(\beta)$, $P_{2X}(\beta)$, and $P_{3X}(\beta)$ are very close to each other especially for those dots of large aspect ratio. Here, P_{3X} refers to the leftmost emission line of the triexciton in order to compare with P_X and P_{2X}. Their difference is seen to become noticeable as the shape of the dots is less anisotropic. Let us first concentrate on the comparison between P_{eh} and P_X. The difference between an exciton and a noninteracting electron-hole pair lies in that the former consists of not only the configuration in which the electron and hole are in their respective ground states but also many other configurations in which the electron and hole are in their excited states, i.e.,

$$X_g = \sum_{i,j} c_{ij} |\Psi_h^i\rangle |\Psi_e^j\rangle, \tag{5}$$

where X_g is the ground state of the exciton. The linear polarization of the emission from a single exciton can then be written as

$$P_X = \frac{\left| \sum_{ij} c_{ij} p_{ij}(x) \right|^2 - \left| \sum_{ij} c_{ij} p_{ij}(y) \right|^2}{\left| \sum_{ij} c_{ij} p_{ij}(x) \right|^2 + \left| \sum_{ij} c_{ij} p_{ij}(y) \right|^2}. \tag{6}$$

If X_g is composed of only the primary configuration $|\Psi_h^g\rangle |\Psi_e^g\rangle$, there would be no difference between P_{eh} and P_X. It is those minor configurations in X_g accounting for the difference, which is a direct result of the correlation effect. While P_{eh} cannot be directly measured in experiments, the correlation effect on the polarization of emission can be identified in the difference among P_X, P_{2X}, and P_{3X}. As the dots become more anisotropic, the multiexciton states are more dominated by their primary configuration. Hence, the correlation effect is seen less important, which explains the relatively less difference among P_{eh} and P_{ex} for the dots of large aspect ratio.

To explore the possibility of optical characterization of structure for self-assembled quantum dots, we calculate the linear polarization of the primary interband transition P_{eh} as a function of the aspect ratio for the dots with various lateral sizes and heights. The result is shown in Fig. 2. The data for P_{ex} are not plotted as they have already been shown to differ very little from P_{eh}.

The ideal situation would be that P_{eh} depends on only the aspect ratio (β) not on the height or lateral size. However, it is seen in reality that the linear polarization of the primary interband transition also depends on other structural parameters. When the height and lateral size are fixed, we find that P_{eh} scales quadratically against the aspect ratio very well. If β is fixed, P_{eh} is seen larger for the thicker dots. If we fix the aspect ratio and height, we see a larger P_{eh} for the bigger dots.

It is worthwhile to mention one interesting relation drawn from the result, i.e., P_{eh} has shown almost the same dependence on β for those dots of similar aspect ratio between the lateral size and height (d/h). For the two different dots, one has a lateral size of 28.8 nm and a height of 5.1 nm ($d/h \approx 5.7$), the other one has 19.8 nm and 3.4 nm ($d/h \approx 5.8$); the calculated P_{eh} is seen to have the same dependence on β. The relation is also found to hold for the other pair; one has $d/h = 28.8/4.0 \approx 7.2$ and the other has $d/h = 19.8/2.8 \approx 7.0$.

It has been shown that the linear polarization of the primary interband transition exhibits a quadratic dependence on the lateral aspect ratio. This dependence is seen also affected by other structural parameters such as the lateral size and height. More importantly, we find that $P_{eh}(\beta)$ exhibits almost the same behavior for those dots of similar aspect ratio between the lateral size and height.

For a dot under strong external excitation, there are many emission lines in the photoluminescence. The polarization of transitions other than the primary one also carries the structural information of the quantum dot. Figure 3 plots the emission spectra of multiexciton complexes up to $6X$ in a dot

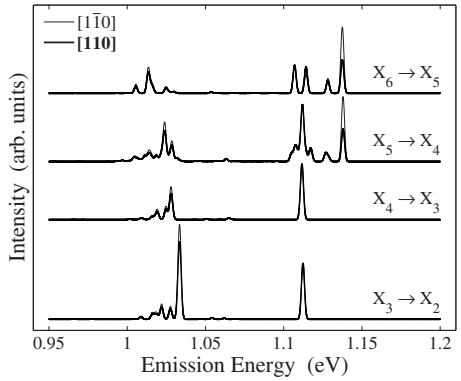

FIG. 3. Emission spectra of multiexciton complexes in a dot of $d=19.8$ nm, $h=2.8$ nm, and $\beta=1.3$.

of an aspect ratio $\beta=1.3$. Let us concentrate on those transitions of the highest energies in each spectrum. While it is surprising to see that the emission lines in $X_4 \rightarrow X_3$ and $X_3 \rightarrow X_2$ exhibit very little anisotropy, $X_5 \rightarrow X_4$ and $X_6 \rightarrow X_5$ are shown to have much larger linear polarization than the single exciton line. Numerically, we find $P_{3X}=0.6\%$, $P_{4X}=1.2\% \ll P_{1X}=10.3\%$, $P_{2X}=10.4\% \ll P_{5X}=33.5\%$, and $P_{6X}=33.1\%$.

The emission lines at the high energy end are the result of recombination of electrons and holes in their excited states. Figure 4 plots the first four confined states in the conduction and valence bands. The first and second excited states of electrons (holes) are found to localized along x and y axes, respectively, which are therefore referred as Ψ_e^x (Ψ_h^x) and Ψ_e^y (Ψ_h^y).

The emission from the single exciton and biexciton involves mostly the ground states of electrons and holes (Ψ_e^g and Ψ_h^g). The effect of higher-lying states has been shown un-noticeable for elongated dots. The emission from triexciton and four-exciton complexes involves the excited states of electrons and holes. In the dots of large aspect ratio, the big energy separation between Ψ_e^x (Ψ_h^x) and Ψ_e^y (Ψ_h^y) results in which ground states of $3X$ and $4X$ are dominated by their primary configurations which consist of mostly Ψ_e^x and Ψ_h^x and very little of Ψ_e^y and Ψ_h^y. The emission lines at the high energy end in $X_3 \rightarrow X_2$ ($X_5 \rightarrow X_4$) and $X_4 \rightarrow X_3$ ($X_6 \rightarrow X_5$) are therefore the result of the recombination of the electronic state Ψ_e^x (Ψ_e^y) and hole state Ψ_h^x (Ψ_h^y).

In the conduction bands, the polarization of the intersubband transitions such as $\Psi_e^g \rightarrow \Psi_e^x$ and $\Psi_e^g \rightarrow \Psi_e^y$ is determined by the direction where the state is localized, i.e., $\Psi_e^g \rightarrow \Psi_e^x$ is

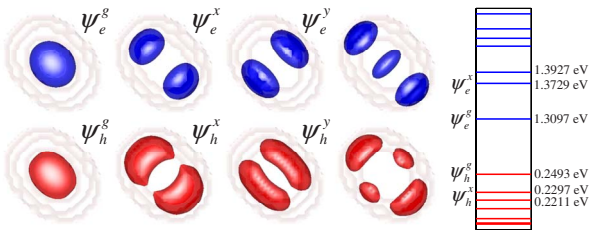

FIG. 4. (Color online) Probability densities (left) and energy levels (right) of the electronic (blue) and hole (red) states in the same dot as in Fig. 3.

almost 100% linearly polarized along the x direction because Ψ_e^x is localized along that direction. It shall be noted that interband transitions are very different from those intersubband transitions. While Ψ_h^x and Ψ_e^x are completely localized along the x direction, transition $\Psi_h^x \rightarrow \Psi_e^x$ exhibits little anisotropy. In the meantime, even though Ψ_h^y and Ψ_e^y are localized along the y direction, transition $\Psi_h^y \rightarrow \Psi_e^y$ shows strong linear polarization along the x direction.

To understand why there is little anisotropy in the emission of $X_4 \rightarrow X_3$ and $X_3 \rightarrow X_2$, we examine the composition of the first and second excited electronic and hole states. In self-assembled quantum dots, the low-lying states in the valence bands are heavy-hole-like states, i.e., their components are mostly $|x\rangle$ and $|y\rangle$ and very little of $|z\rangle$. At the presence of the mixing between the conduction and valence bands, $|s\rangle$ should also be taken into account. We have

$$\begin{aligned}
\Psi_h^x &= \Psi_h^{xs}|s\rangle + \Psi_h^{xx}|x\rangle + \Psi_h^{xy}|y\rangle, \\
\Psi_h^y &= \Psi_h^{ys}|s\rangle + \Psi_h^{yx}|x\rangle + \Psi_h^{yy}|y\rangle, \\
\Psi_e^x &= \Psi_e^{xs}|s\rangle + \Psi_e^{xx}|x\rangle + \Psi_e^{xy}|y\rangle, \\
\Psi_e^y &= \Psi_e^{ys}|s\rangle + \Psi_e^{yx}|x\rangle + \Psi_e^{yy}|y\rangle. \qquad (7)
\end{aligned}$$

The momentum matrix elements among these states are then given by

$$\begin{aligned}
&p_{h_x,e_x}(x) \propto \langle \Psi_h^{xx}|\Psi_e^{xs}\rangle, \quad p_{h_x,e_x}(y) \propto \langle \Psi_h^{xy}|\Psi_e^{xs}\rangle, \\
&p_{h_y,e_y}(x) \propto \langle \Psi_h^{yx}|\Psi_e^{ys}\rangle, \quad p_{h_y,e_y}(y) \propto \langle \Psi_h^{yy}|\Psi_e^{ys}\rangle. \qquad (8)
\end{aligned}$$

Approximately, the linear polarization of the multiexciton emission can then be written as

$$\begin{aligned}
P_{3X} = P_{4X} &= \frac{|p_{h_x,e_x}(x)|^2 - |p_{h_x,e_x}(y)|^2}{|p_{h_x,e_x}(x)|^2 + |p_{h_x,e_x}(y)|^2}, \\
P_{5X} = P_{6X} &= \frac{|p_{h_y,e_y}(x)|^2 - |p_{h_y,e_y}(y)|^2}{|p_{h_y,e_y}(x)|^2 + |p_{h_y,e_y}(y)|^2}. \qquad (9)
\end{aligned}$$

Hence, we can see that the polarization of the multiexciton emission originates from the polarized component profile of the corresponding states in the valence bands. Quantitatively, we can define the polarization of components in the states Ψ_h^x and Ψ_h^y as

$$\begin{aligned}
P_{\Psi_h^x} &= \frac{|\langle \Psi_h^{xx}|\Psi_h^{xx}\rangle|^2 - |\langle \Psi_h^{xy}|\Psi_h^{xy}\rangle|^2}{|\langle \Psi_h^{xx}|\Psi_h^{xx}\rangle|^2 + |\langle \Psi_h^{xy}|\Psi_h^{xy}\rangle|^2}, \\
P_{\Psi_h^y} &= \frac{|\langle \Psi_h^{yx}|\Psi_h^{yx}\rangle|^2 - |\langle \Psi_h^{yy}|\Psi_h^{yy}\rangle|^2}{|\langle \Psi_h^{yx}|\Psi_h^{yx}\rangle|^2 + |\langle \Psi_h^{yy}|\Psi_h^{yy}\rangle|^2}. \qquad (10)
\end{aligned}$$

If the components $|x\rangle$ and $|y\rangle$ have similar probability density distribution in the states Ψ_h^x and Ψ_h^y, to a good degree of approximation, we have $P_{3X}=P_{4X} \approx P_{\Psi_h^x}$ and $P_{5X}=P_{6X} \approx P_{\Psi_h^y}$.

Figure 5 plots the composition profile of the first two excited states in the valence bands. It is seen that the first excited state Ψ_h^x has much less polarized components than the other state Ψ_h^y, i.e., $P_{\Psi_h^x}(\beta) \ll P_{\Psi_h^y}(\beta)$. This explains why

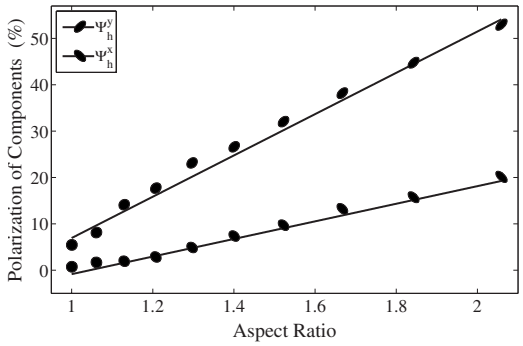

FIG. 5. Polarization of components in the valence-band states Ψ_h^x and Ψ_h^y, as defined in Eq. (10), calculated as a function of the aspect ratio for the dots of $d=19.8$ nm and $h=2.8$ nm. Linear fit is shown in solid lines.

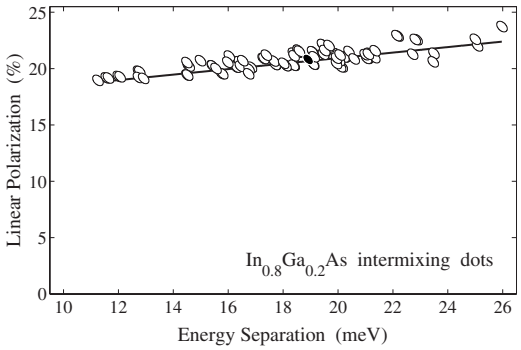

FIG. 6. Linear polarization of the primary interband transition, depicted in open dots, as a function of the energy split between the first two excited electronic states calculated for $In_{0.8}Ga_{0.2}As$ quantum dots of random intermixing profile. Linear fit to the data is shown in the solid line. The result for the dot of a homogeneous composition profile is plotted in the solid dot.

the rightmost emission lines in $X_4 \rightarrow X_3$ and $X_3 \rightarrow X_2$ exhibit very small anisotropy even in a dot of a large degree of elongation. Numerically, we find $P_{\Psi_h^x}=4.1\%$ and $P_{\Psi_h^y}=22.5\%$ at $\beta=1.3$. The noticeable difference between $P_{\Psi_h^y}$ and P_{5X} or P_{6X} is due to which $P_{\Psi_h^{yx}}$ and $P_{\Psi_h^{yy}}$ have very different probability density distribution.

When a dot is elongated, the energy separation between the first two electronic and hole excited states would be increased. In Fig. 3, the separation between the rightmost emission lines in $X_4 \rightarrow X_3$ and $X_5 \rightarrow X_4$ becomes a good approximation to $(E_{e_y}-E_{e_x})+(E_{h_y}-E_{h_x})$ if the aspect ratio is large enough. In experiments, these emission lines can be easily identified by their power dependence, and the energy split is often used to characterize the geometric anisotropy of quantum dots.[15] However, such a separation is not necessarily induced by the shape anisotropy. For example, random intermixing effect may cause a large separation between these states.

Figure 6 plots the linear polarization of the primary interband transition as a function of the electronic energy split for 100 quantum dots of random intermixing profile. Each dot has fixed $d=28.8$ nm, $h=5.1$ nm, and $\beta=1.5$. The result for the dot of a homogeneous composition profile is shown in a solid dot. It can be seen that the random intermixing effect may induce a large variation in the energy split, while it does not affect much on the optical anisotropy. The standard deviation for the linear polarization is found less than 5.0%. It can therefore be concluded that optical anisotropy, precisely the linear polarization of the primary interband transition, can be used for characterizing the geometric anisotropy of quantum dots.

In conclusion, we have studied the linear polarization of the multiexciton emission from self-assembled quantum dots by using an empirical tight-binding method. We have found that the electron-electron interaction has little effect on the polarization of the primary interband transition. The polarization property is also shown to be insensitive to the random intermixing effect, which makes it an appropriate tool for characterizing structure for quantum dots. The transitions at the high energy end in the spectra are found to exhibit very different polarization property from the primary interband transition, which we attribute to the different component profiles in the excited hole states.

This work is supported by the NSFC (No. 10634040, No. 10644001, and No. 10774025), the 973 projects of MOST of China (No. 2004CB619004 and No. 2006CB921506), the STCSM (No. 07pj14010), and the HK RGC-CERG Grant under Contract No. HKU 7049/04P.

[1] L. Jacak, P. Hawrylak, and A. Wojs, *Quantum Dots* (Springer, Berlin, 1998).
[2] D. Bimberg, M. Grundmann, and N. N. Ledentsov, *Quantum Dot Heterostructures* (Wiley, New York, 1998).
[3] V. Zwiller, L. Jarlskog, M.-E. Pistol, C. Pryor, P. Castrillo, W. Seifert, and L. Samuelson, Phys. Rev. B **63**, 233301 (2001).
[4] I. Favero, G. Cassabois, A. Jankovic, R. Ferreira, D. Darson, C. Voisin, C. Delalande, Ph. Roussignol, A. Badolato, P. M. Petroff, and J. M. Gérard, Appl. Phys. Lett. **86**, 041904 (2005).
[5] S. Cortez, O. Krebs, P. Voisin, and J. M. Gerard, Phys. Rev. B **63**, 233306 (2001).
[6] A. V. Koudinov, I. A. Akimov, Yu. G. Kusrayev, and F. Henneberger, Phys. Rev. B **70**, 241305(R) (2004).
[7] W. Sheng, Appl. Phys. Lett. **89**, 173129 (2006).
[8] S. Raymond *et al.* Phys. Rev. Lett. **92**, 187402 (2004).
[9] S. Lee, L. Jönsson, J. W. Wilkins, G. W. Bryant, and G. Klimeck, Phys. Rev. B **63**, 195318 (2001).
[10] W. Jaskólski, M. Zieliński, G. W. Bryant, and J. Aizpurua, Phys. Rev. B **74**, 195339 (2006).
[11] W. Sheng, S.-J. Cheng, and P. Hawrylak, Phys. Rev. B **71**, 035316 (2005).
[12] G. Bester, S. Nair, and A. Zunger, Phys. Rev. B **67**, 161306(R) (2003).
[13] G. A. Narvaez, G. Bester, and A. Zunger, Phys. Rev. B **72**, 245318 (2005).
[14] R. Seguin, A. Schliwa, S. Rodt, K. Pötschke, U. W. Pohl, and D. Bimberg, Phys. Rev. Lett. **95**, 257402 (2005).
[15] S. Hameau, Y. Guldner, O. Verzelen, R. Ferreira, G. Bastard, J. Zeman, A. Lemaitre, and J. M. Gerard, Phys. Rev. Lett. **83**, 4152 (1999).